Int J Adv Manuf Technol (2010) 48:513–528
DOI 10.1007/s00170-009-2307-1

ORIGINAL ARTICLE

Optimization and prediction of weldment profile in bead-on-plate welding of Al-1100 plates using electron beam

Vidyut Dey · Dilip Kumar Pratihar · Gouranga L. Datta · M. N. Jha · T. K. Saha · A. V. Bapat

Received: 13 March 2009 / Accepted: 9 September 2009 / Published online: 23 September 2009

Abstract Bead-on-plate welds were carried out on aluminum plates Al-1100 using an electron beam welding machine. The weld runs were conducted as per central composite design. Regression analysis was then carried out to establish input–output relationships of the process. The weldment area was minimized, after satisfying the condition of maximum bead penetration. The above constrained optimization problem was solved utilizing a genetic algorithm (GA) with a penalty function approach. The GA was able to determine optimal weld-bead geometry and recommend the necessary process parameters for the same. An attempt was also made to model the complicated dagger-like profile of electron-beam welded material by utilizing three third-order curves. The profiles were predicted by utilizing both back-propagation trained and GA-tuned neural networks. The latter was able to yield better predictions compared to the former.

Keywords Electron beam welding · Optimization · Genetic algorithm · Bead profile prediction · Neural networks

V. Dey · D. K. Pratihar (✉) · G. L. Datta
Department of Mechanical Engineering,
Indian Institute of Technology, Kharagpur, 721 302, India
e-mail: dkpra@mech.iitkgp.ernet.in

M. N. Jha · T. K. Saha · A. V. Bapat
BARC, Mumbai, India

1 Introduction

Electron beam welding (EBW) is a process wherein required parts are fabricated by fusing the base metals with the heat obtained from a concentrated beam composed primarily of high-velocity electrons [1]. The kinetic energy of these high-velocity electrons is changed to thermal energy, upon striking the surfaces to be joined, thereby melting and fusing the workpiece metal. The main advantage of this autogenous process lies in the fact that it can produce deep and narrow welds. The welded structure is monolithic, which may be divided into three distinct zones, namely, (1) fusion zone, (2) heat-affected zone (HAZ), and (3) un-affected zone. Out of these, the fusion zone and HAZ undergo metallurgical changes. The mechanical properties of the welded structure depend upon the metallurgical features present in both the fusion and HAZ. Thus, the size and shape of the fusion zone has got implication over the metallurgical properties. The shape of the weldment in EBW is generally found to be different from those formed with conventional welding processes. The shapes in conventional welding processes are seen to be parabolic, whereas in case of EBW, it is found to have a dagger-like structure due to the key-hole formation. The operating parameters of the process influence the shape of the weldment. Thus, the mechanical properties, to a large extent, are also governed by the shape and size of the weldment. The conventional method of specifying the bead geometry of a weldment is in terms of its height, width, and penetration. Specifying the bead shape in terms of the above features may carry some incomplete information but does not highlight the contour of the weldment.

2 Literature review

EBW, like any other welding technique, has various control parameters. Accelerating voltage, beam current, welding speed, vacuum level in the chamber, and distance of the focal point from the workpiece surface are some of the parameters that need to be controlled during the welding. Various researchers have tried several techniques to relate these variables to the bead geometry of the weldment. Koleva [2] used multi-response statistical techniques to predict the depth and width of the beads while welding stainless steel. Koleva [3] utilized thermal efficiency in connection with the bead-geometric parameters. In this study, bead penetration and width were formulated as a function of thermal efficiency of the process. Since there are too many parameters involved in a welding process, Gunaraj and Murugan [4, 5] studied the main and interaction effects of the process control variables on bead-geometric parameters using non-linear regression models. Although the authors used non-linear regression methods, it was established by Yang et al. [6] that linear regression equations could give correlation coefficients similar to those obtainable from the curvilinear regression equations. It is generally seen that the above statistical regression analysis gives satisfactory results to predict the anchor points only. However, there might be some significant deviations in prediction at the intermediate points, particularly near the center. To overcome this problem, Ganjigatti et al. [7] developed a new methodology to model the input–output relationships by carrying out regression analysis cluster-wise, which took care of the forecasting of intermediate points, as well. The non-linearity aspect amongst the various factors was solved by Benyounis et al. [8] with the help of response surface methodology to predict the weld-bead profile.

The welding process is a very complicated phenomenon, and its variables generally have highly non-linear relationships with one another. Non-linearity to this extent cannot be very well-defined by a fixed-order regression equation. To overcome this, some investigators tried to model the input–output relationships using neural networks. Nagesh and Datta [9] used a back-propagation neural network to predict the bead geometries of mild steel electrodes deposited on cast iron plates. De et al. [10] used artificial neural network (ANN) to predict the quality of welding in the pulsed-current gas metal arc welding (GMAW) process. Kim et al. [11] showed that a neural network-based model could give better prediction of the bead height than the empirically developed equations could do. In a similar fashion, it was shown by Lee and Um [12] that the neural network could predict back the bead geometries better than the empirical relationships developed by the regression analysis did. Ping et al. [13] modified the structure of a conventional feed-forward multi-layer perceptron network with a single output instead of the multi-outputs. This type of network was named self-adaptive offset network (SAON). The authors proved that SAON could work better than the conventional networks.

Several attempts were also made by various researchers to optimize the weld-bead geometry. Tay and Butler [14] used a radial basis function to approximate stochastically the non-linear dynamics of the welding process, in order to optimize the basic welding parameters. In welding, where filler materials are used, not only the bead-geometric parameters, but also the total volume of metal added for welding is important from a quality point of view, as it adds on to the cost. Gunaraj and Murugan [15] considered the volume of the electrode to be a parameter and then utilized the optimization tool of MATLAB to optimize the volume of the weldment. Tarng and Yang [16] used the Taguchi method to conduct their experiments with the gas tungsten arc (GTA) welding process. The Taguchi method was then systematically and efficiently used for searching the welding process parameters with an optimal weld-bead geometry. The optimal weld-bead geometry had the-smaller-the-better quality characteristics for the front height, front width, back height, and back width of the weld bead. A slight variation to this method will give rise to the Grey-based Taguchi method [17], in which a Grey relational grade was obtained. This was used to evaluate the multiple performance outputs, and thus, complicated multiple performance characteristics could be converted into the optimization of a single Grey relational grade. Olabi et al. [18] utilized an ANN to generate suitable welding data necessary to optimize the welding parameters of CO_2 laser by Taguchi method, so that the maximum ratio of weld depth to width could be obtained.

To optimize the welding parameters, Kim et al. [19] developed a technique called controlled random search (CRS), where the near-optimal settings of the welding process parameters were determined through the experiments conducted as per the response surface methodology (RSM). The objective function of RSM need not be differentiable. The parameters of welding were also optimized using a genetic algorithm (GA) [20]. In cases where the search space is large and the objective functions become highly complicated, the computational time of a GA increases drastically and

it becomes difficult to get any solution in real time. To overcome this difficulty, Kumar and Debroy [21] and Mishra and Debroy [22] showed that multiple sets of welding variables capable of producing the target weld geometry could be determined in a realistic time frame by coupling a real-coded GA with a neural network model.

During welding, disturbances and changes in the welding working environment lead to variations in the output variables associated with the weld quality. To enhance the weld quality, it is essential to optimize the welding process by taking both the variance and average value of the output variables into consideration. Kim et al. [23] used a *dual response approach* to determine the welding process parameters, which could produce the target value with minimal variance. The dual response approach could optimize the penetration in GMA welding. The regression models for the mean values and standard deviations of the penetration were developed first, and subsequently, an optimization algorithm was applied based on the regression models and constraints to determine the welding process parameters that generated the desired penetration with the minimized variance.

Application of the GA in tandem with a neural network was shown in the form of comparative studies of back-propagation neural network (BPNN) and GA-tuned NN (GANN) by various investigators. Dutta and Pratihar [24] compared the results of regression analysis, BPNN, and GANN for modeling the bead geometries of a TIG welding process and found the GANN to perform better than both the BPNN and regression analysis. Moreover, Mollah and Pratihar [25] determined input–output relationships of the TIG welding process using the radial basis function neural networks (RBFNNs).

Some attempts were also made to predict the weld bead profile. Kim et al. [26] tried to predict the parabolic weld bead profile of GMA with the help of *penetration shape factor*, *reinforcement shape factor*, etc. Peretz [27] developed a mathematical model based on heat transfer to predict the capillary shape and weld cross-section profile in case of laser beam welding. Dimensionless numbers like *Peclet numbers* and *Marangoni numbers* [28, 29] were used to predict the shapes of the knives obtained as the bead profile. A preliminary attempt was made by Dey et al. [30] to determine optimal weld bead geometry and its corresponding optimized set of input parameters for carrying out bead-on-plate welding on stainless steel plates. However, no attempt was made in that work to predict the contour of the weldment.

In the present study, bead-on-plate welding has been carried out on aluminum plates of size 75 × 30 × 12 mm, as per central composite design of experiments using an EBW technique. The weld-bead geometry has been optimized using a GA along with a penalty function approach for handling the constraints. An attempt has also been made to predict the contour of the weldment for a set of input process parameters.

3 Problem formulation and proposed methods of solution

Figure 1 shows the schematic view of a weld bead geometry. No filler material is used in the EBW. Thus, it is an autogenous process, and consequently, no reinforcement is generally found at the top of the bead. Only the geometric parameters like bead width and penetration were measured during the data collection. Weld profiles were divided into three parts. For each etched specimen, a_1, b_1, a_2, b_2, BW, and BP were measured. The weldment was found to have a dagger-like shape. The area of the weldment was estimated mathematically, which depends on both BW and BP. A GA with a penalty function approach was utilized to determine the parameters required for obtaining the minimum weldment area, after ensuring the maximum penetration. As the weldment had a complex geometry,

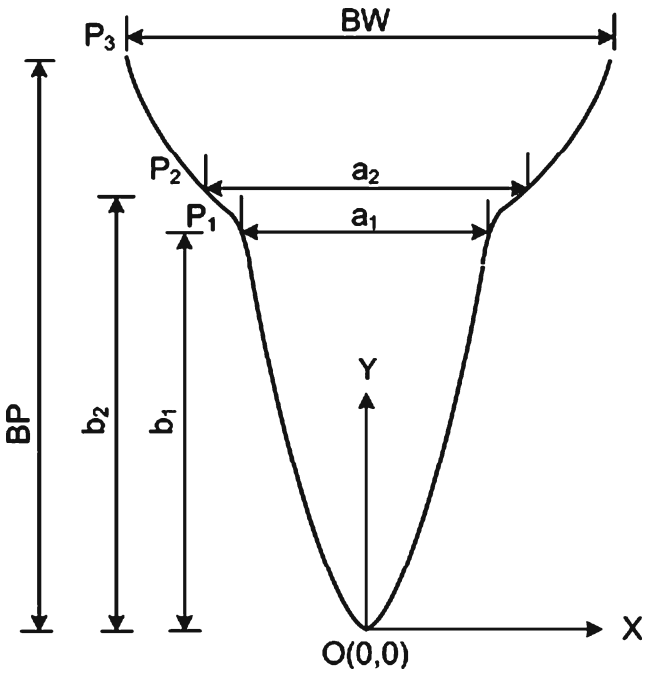

Fig. 1 A schematic view of weld bead geometry

six third-order curves were utilized to represent the same. Neural network-based models were also developed to predict the weld bead profile.

3.1 Application of a GA to minimize the weldment area

GA, introduced by John Holland [31], is a population-based search and optimization tool. The GA works equally good in either continuous or discrete search space. It is a heuristic technique inspired by the natural evolutionary process comprising of a few operators, namely selection, crossover, mutation, and others. The evolution starts with a population of randomly generated individuals in the first generation. In every generation, the fitness of each individual in the population is evaluated, compared with the best value, and modified (recombined and possibly randomly mutated), if required, to form a new population of solutions. The new population is then used in the next iteration of the algorithm. The algorithm terminates when either a maximum number of generations has been produced or a satisfactory fitness level has been reached for the population. Figure 2 shows the working cycle of a GA.

Each side of the weldment (as shown in Fig. 1), was supposed to be comprised of three third-order curves. The equations representing the weldment can be written as follows:

$$Y = A_{10} + A_{11}x + A_{12}x^2 + A_{13}x^3 \tag{1}$$

$$Y = A_{20} + A_{21}x + A_{22}x^2 + A_{23}x^3 \tag{2}$$

$$Y = A_{30} + A_{31}x + A_{32}x^2 + A_{33}x^3 \tag{3}$$

where A_{10}, A_{11}, A_{12}, A_{13}, A_{20}, A_{21}, A_{22}, A_{23}, A_{30}, A_{31}, A_{32}, and A_{33} were the co-efficients to be determined. The above equations were subjected to various boundary conditions. The coefficients were determined by solving 12 equations after putting the boundary conditions. The equations are shown below in a matrix form.

$$\begin{bmatrix}
1 & 0 & 0 & 0 & 0 & 0 & 0 & 0 & 0 & 0 & 0 & 0 \\
0 & 1 & 0 & 0 & 0 & 0 & 0 & 0 & 0 & 0 & 0 & 0 \\
1 & \left(\frac{a_1}{2}\right) & \left(\frac{a_1}{2}\right)^2 & \left(\frac{a_1}{2}\right)^3 & 0 & 0 & 0 & 0 & 0 & 0 & 0 & 0 \\
0 & 0 & 0 & 0 & \left(\frac{a_1}{2}\right) & \left(\frac{a_1}{2}\right)^2 & \left(\frac{a_1}{2}\right)^3 & 0 & 0 & 0 & 0 & 0 \\
0 & 1 & 2\left(\frac{a_1}{2}\right) & 3\left(\frac{a_1}{2}\right)^2 & 0 & -1 & -2\left(\frac{a_1}{2}\right) & -3\left(\frac{a_1}{2}\right) & 0 & 0 & 0 & 0 \\
0 & 0 & 2 & 6\left(\frac{a_1}{2}\right) & 0 & 0 & -2 & -6\left(\frac{a_1}{2}\right) & 0 & 0 & 0 & 0 \\
0 & 0 & 0 & 0 & 1 & \left(\frac{a_2}{2}\right) & \left(\frac{a_2}{2}\right)2 & \left(\frac{a_2}{2}\right)^3 & 0 & 0 & 0 & 0 \\
0 & 0 & 0 & 0 & 0 & 0 & 0 & 0 & 1 & \left(\frac{a_2}{2}\right) & \left(\frac{a_2}{2}\right)^2 & \left(\frac{a_2}{2}\right)^3 \\
0 & 0 & 0 & 0 & 0 & 1 & 2\left(\frac{a_2}{2}\right) & 3\left(\frac{a_2}{2}\right)^2 & 0 & -1 & -2\left(\frac{a_2}{2}\right) & -3\left(\frac{a_2}{2}\right)^2 \\
0 & 0 & 0 & 0 & 0 & 0 & 2 & 6\left(\frac{a_2}{2}\right) & 0 & 0 & -2 & -6\left(\frac{a_2}{2}\right) \\
0 & 0 & 0 & 0 & 0 & 0 & 0 & 0 & 1 & \left(\frac{\mathrm{BW}}{2}\right) & \left(\frac{\mathrm{BW}}{2}\right)^2 & \left(\frac{\mathrm{BW}}{2}\right)^3 \\
0 & 0 & 0 & 0 & 0 & 0 & 0 & 0 & 0 & 1 & 2\left(\frac{\mathrm{BW}}{2}\right) & 3\left(\frac{\mathrm{BW}}{2}\right)^2
\end{bmatrix} = \begin{bmatrix} 0 \\ 0 \\ b_1 \\ b_1 \\ 0 \\ 0 \\ b_2 \\ b_2 \\ 0 \\ 0 \\ \mathrm{BP} \\ 0 \end{bmatrix} \tag{4}$$

The fitness f of the GA solution was expressed as the area of the weld profile bound within the six curves representing the contour of the weldment. The GA will try to minimize the weldment area, after ensuring a maximum value of the bead penetration. A penalty function approach was utilized to solve the said constrained optimization problem. In this approach, the fitness function of a solution (say i-th) is expressed by modifying its objective function as follows: $F_i(\mathrm{X}) = f_i(\mathrm{X}) \pm P_i$, where P_i indicates the penalty used to penalize an infeasible solution. For a feasible solution, P_i was set equal to 0.0, whereas, for an infeasible solution, P_i was expressed

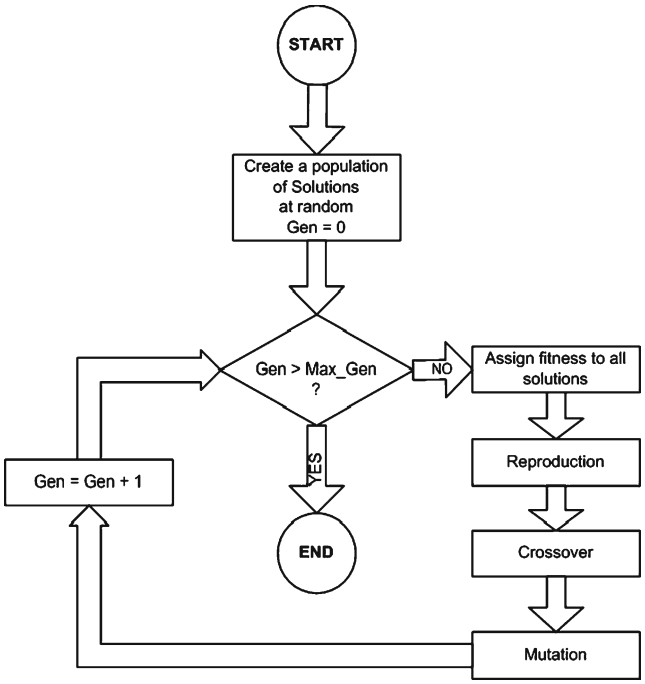

Fig. 2 Working cycle of a GA

like the following: $P_i = C \sum_{k=1}^{q} \{\phi_{ik}(X)\}^2$, where C indicates the user-defined penalty coefficient and $\{\phi_{ik}(X)\}^2$ represents the penalty term for the k-th constraint, corresponding to the i-th objective function. The penalties can be either *static*, *adaptive*, or *dynamic* in nature. For a further detailed discussion on the working principle of the GA, interested readers may refer to the works of Chakrabori [32] and Pratihar [33].

In this study, the aim was to optimize the welding operating parameters, so that the area of the weldment could be minimized subject to maximizing the weld penetration. The weldment area was assumed to be symmetric about the center line. For the sake of simplicity, the origin of the co-ordinate system was assumed to be at the bottom center of the curve.

The above constrained optimization problem was mathematically stated as follows:

Minimize weldment area

subject to the condition that BP takes the maximum value and

$$V_{min} \leq V \leq V_{max},$$
$$I_{min} \leq I \leq I_{max},$$
$$S_{min} \leq S \leq S_{max}.$$

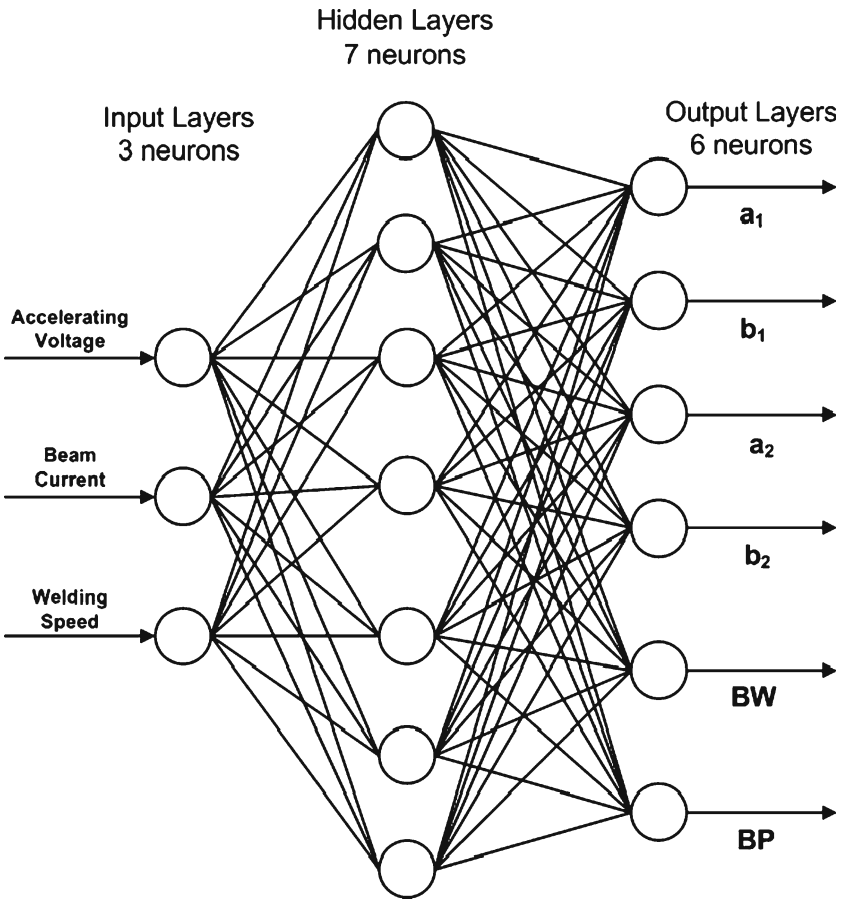

Fig. 3 A schematic view of a neural network

A binary-coded GA was used to solve the above optimization problem. The fitness f of the GA solution was expressed as the area of the weld profile bound within the six curves. The minimum value of BW and maximum value of BP may be obtained by varying the input process parameters, that is, V, I, and S within their respective ranges. The GA will try to minimize the weldment area by pushing the values of both BW and BP towards their respective minimum values. However, the aim of the present study is to minimize the weldment area by maximizing the BP. To solve the said problem, the concept of penalty term was used. If the above condition was not maintained by a GA solution, its fitness value was penalized by using a term given below.

$$\mathrm{P} = \mathrm{C} \times \left[\left(\frac{\mathrm{BW}}{\mathrm{BW_{min}}} \right)^{\mathrm{a}} + \left(\frac{\mathrm{BP_{max}}}{\mathrm{BP}} \right)^{\mathrm{b}} \right], \tag{5}$$

where a, b, and C were non-negative numbers, whose values were determined through a careful study.

3.2 Application of BPNN and GANN to predict the weldment profile

Each side of the curve was assumed, intuitively, to be consisting of three different curves. The endpoints of the curves (as shown in Fig. 1) are denoted by O, P_1; P_1, P_2; and P_2, P_3, respectively. The coordinates of three points, P_1, P_2, and P_3, were $\left(\frac{a_1}{2}, b1\right)$, $\left(\frac{a_2}{2}, b2\right)$, and $\left(\frac{\mathrm{BW}}{2}, \mathrm{BP}\right)$, respectively. The symbols: BP and BW represent bead penetration and width, respectively. The values of the above coordinates for all 51 (i.e., 17×3) cases were measured and utilized in deriving the regression equations. The equations were then used to generate 1,000 test cases at random, which were

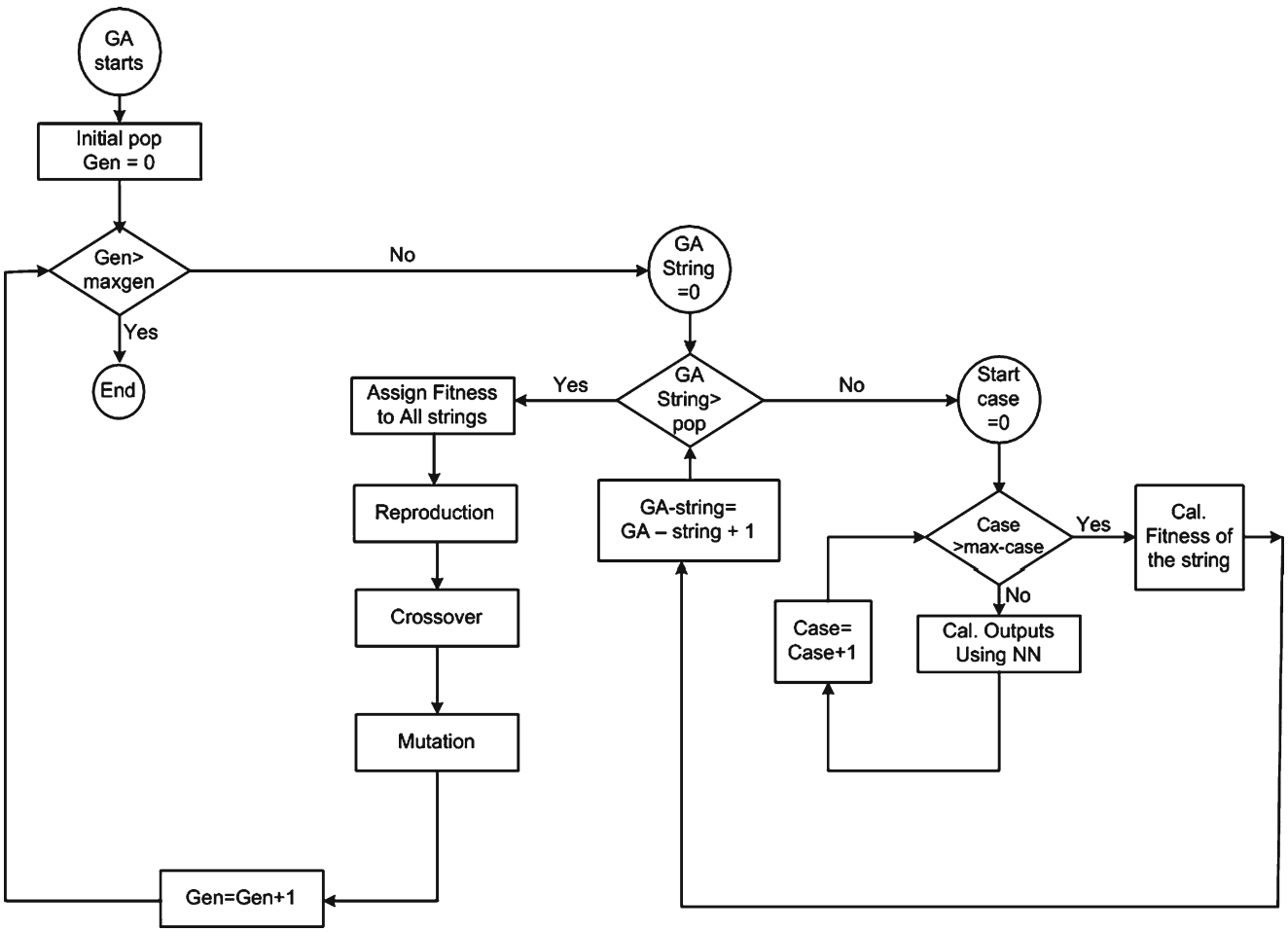

Fig. 4 A schematic view showing the working cycle of a GA-NN

Table 1 Composition of Al-1100

Al	Si	Fe	Cu	Mn	Mg	Ti	Cr	Ni	B	Zr	V	Sb	Ga	P
98.8694	0.45827	0.13617	0.00983	0.47047	0.01191	0.00083	0.00066	0.00039	0.00039	0.00095	0.00630	0.00059	0.01506	0.00095

utilized to train the network. A neural network (refer to Fig. 3) was used to predict the outputs. The network consisted of three layers, namely, input, hidden, and output. Three inputs were considered in the input layer, namely, accelerating voltage (V), beam current (I), and welding speed (S). The output layer had six neurons carrying information of a_1, b_1, a_2, b_2, BW, BP. The hidden layer had seven neurons. The neurons of the input, hidden, and output layers were assumed to have the linear, log-sigmoid, and log-sigmoid transfer functions, respectively. A fixed value of bias $b = 0.00009505$ was added to all the neurons. The connecting weights between the input and hidden layers were represented by $[V]$, and those between the hidden and output layers were denoted by $[W]$. The values of $[V]$ and $[W]$ lie in the range of 0.0 to 1.0, whose initial values were generated at random. A batch mode of training had been adopted. Mean squared deviation (MSD) in prediction denoted by E was calculated as follows:

$$E = \frac{1}{S}\sum_{s=1}^{S}\frac{1}{M}\sum_{m=1}^{M}\frac{1}{2}\left(T_{om}^{s} - O_{om}^{s}\right), \tag{6}$$

where S denotes the number of training cases, M represents the number of outputs, T_{om}^{s} is the target output of the m^{th} neuron lying on the output layer corresponding to the s^{th} training case, and O_{om}^{s} represents the predicted output of the m^{th} neuron lying on the output layer corresponding to the s^{th} training case. The connecting weights $[V]$ and $[W]$ were updated to reduce the error E during the training of the network.

In the genetic-neural system (GA-NN), the error in prediction of the network was minimized by using a GA, in place of the back-propagation algorithm. A GA-string carries information of the weight values, coefficient of transfer functions, etc. The schematic view of the GA-NN scheme is shown in Fig. 4. A batch mode of training was adopted, where the whole training set was passed through a neural network represented by a GA string. The fitness function f of the GA was expressed using the same expression of mean squared deviation in prediction given in Eq. 6. The population of GA strings was then modified using the operators like reproduction, crossover, and mutation. The number of hidden neurons and bias value were kept the same as those used in the BPNN. The GA string was found to be 1,360 bits long. *Tournament- selection* scheme was adopted in the model. A *uniform-crossover* scheme had been utilized in the GA.

4 Experimental data collection

Bead-on-plate welding experiments were conducted on a 24-kW EBW machine, indigenously developed at CDM, Bhabha Atomic Research Centre, Mumbai, India. Welding was carried out on Al-1100 plates, whose chemical compositions are shown in Table 1. Three parameters, namely, accelerating voltage, beam current, and welding speed were varied during the experiments. Three levels, such as the maximum, minimum, and mid-value, were considered for each input process parameter, the details of which are shown in Table 2. A central composite design (CCD) was obtained, in which $2^3 + 2 \times 3 + 3 = 17$ combinations of input process parameters were considered to conduct the experiments. As three replicates were considered for each combination of input parameters, a total of $3 \times 17 = 51$ experiments were conducted. The welded specimens were cut along the cross sections. They were then polished and etched to reveal the weldment area.

Table 2 Input process parameters and their ranges

Inputs	Units	Coded symbol	Un-coded symbol	Minimum value	Mid-value value	Maximum value
Acc. voltage	kV	X_1	V	60	75	90
Beam current	mA	X_2	I	30	40	50
Weld speed	mm/min	X_3	S	1,000	1,200	1,400

The specimens were then scanned in a scanner to 12 times of their sizes.

5 Results and discussion

Results related to conventional regression analysis, optimization of weld bead geometry, and prediction of the bead profile are stated and discussed below.

5.1 Regression analysis

Non-linear regression analysis was carried out to establish input–output relationships of the process. The obtained response equations are shown below.

5.1.1 Bead penetration

Equation 7 shows the regression equation for bead penetration, expressed in its coded form.

$$\begin{aligned} \mathrm{BP}_{\mathrm{coded}} = {} & 5.65913 + 1.68014X_1 + 1.86107X_2 \\ & - 0.49440X_3 + 0.07801X_1^2 \\ & + 0.14402X_2^2 - 0.06054X_3^2 \\ & + 0.33712X_1X_2 - 0.24639X_1X_3 \\ & + 0.01007X_2X_3 \end{aligned} \tag{7}$$

A significance test was carried out to investigate the contribution of process parameters on the said response. It was observed that the parameters X_1, X_2, X_3, X_2^2, X_1X_2, and X_1X_3 had significant contributions on BP (refer to Table 3). It is important to mention that a correlation coefficient of 0.993 was obtained for this response. The lack of fit, as shown in Table 4, was found to be significant.

The inter-relationships among various working parameters and the responses were better revealed in the surface plots, as shown in Fig. 5. Bead penetration

Table 3 Significance test for BP

Sl. no.	Term	Coeff	SE coeff	T	p
1	Constant	5.65913	0.04746	119.228	0.000
2	X_1	1.68014	0.03508	47.898	0.000
3	X_2	1.86107	0.03508	53.056	0.000
4	X_3	−0.49440	0.03508	−14.094	0.000
5	X_1^2	0.07801	0.06777	1.151	0.256
6	X_2^2	0.14402	0.06777	2.125	0.040
7	X_3^2	−0.06054	0.06777	−0.893	0.377
8	X_1X_2	0.33712	0.03922	8.596	0.000
9	X_1X_3	−0.24639	0.03922	−6.283	0.000
10	X_2X_3	0.01007	0.03922	0.257	0.799

$S = 0.1921$ $R^2 = 99.3\%$ $R^2(\mathrm{adj}) = 99.1\%$

Table 4 ANOVA test for BP

Source	DF	Seq SS	Adj SS	Adj MS	F	p
Regression	9	200.462	200.462	22.2736	603.41	0.000
Linear	3	195.927	195.927	65.3089	1,769.28	0.000
Square	3	0.349	0.349	0.1162	3.15	0.035
Interaction	3	4.187	4.187	1.3957	37.81	0.000
Residual error	41	1.513	1.513	0.0369		
Lack-of-fit	5	0.696	0.696	0.1392	6.13	0.000
Pure error	36	0.817	0.817	0.0227		
Total	50	201.976				

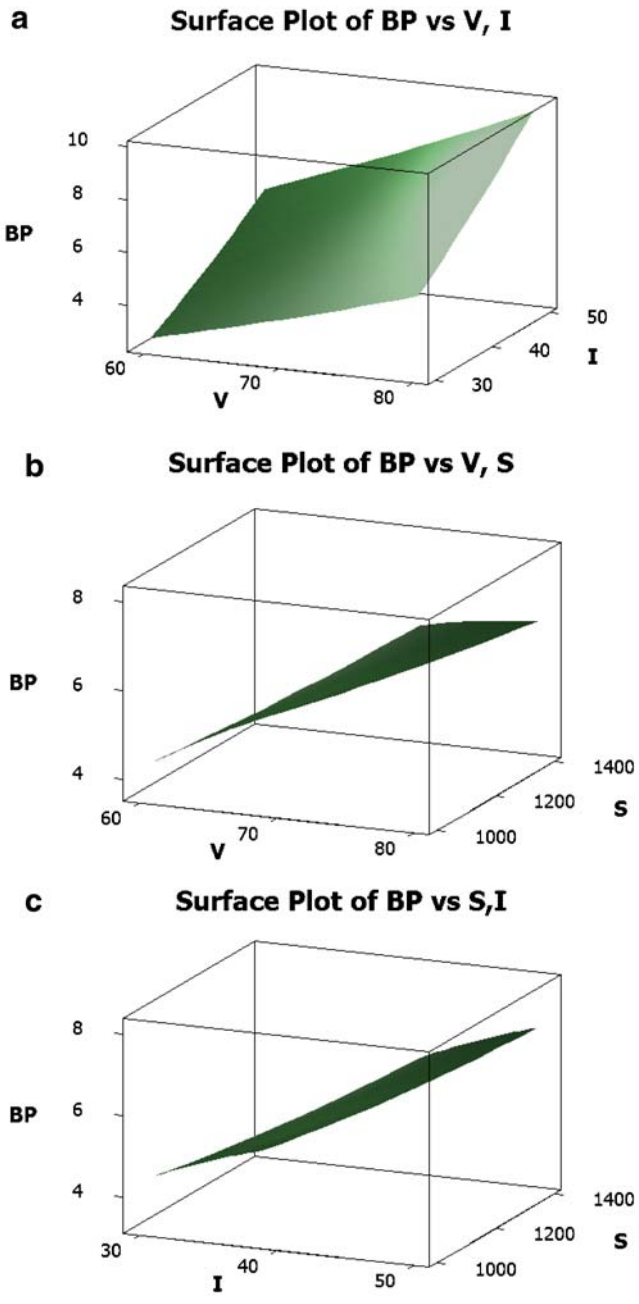

Fig. 5 Surface plots of BP with V, I, and S (**a**–**c**)

was found to increase with the increase in accelerating voltage and beam current, whereas it reduced with the increase in welding speed. Thus, it may be concluded that, in order to get the maximum bead penetration, the welding should be done at a lower welding speed and higher accelerating voltage and beam current. The above observation exactly matches with that of Table 3. The un-coded form of BP was found to be as follows:

$$\begin{aligned}\mathrm{BP}_{\mathrm{un-coded}} = {} & -7.29937 + 0.0717787V - 0.171138I \\ & + 0.00958261S + 0.000780140V^2 \\ & + 0.00144023I^2 - 0.00000151356S^2 \\ & - 0.00337119VI - 0.000123193VS \\ & - 0.00000503661IS \end{aligned} \quad (8)$$

The performance of the developed model was tested on eight cases. The model-predicted BP were compared with its experimental values for eight test cases and the values of percentage deviation in prediction were computed. Figure 6 shows the values of percentage deviation in prediction of BP for the said cases. It is important to note that the values of percentage deviation in prediction of BP were lying between −28.15% and 2.30%.

5.1.2 Bead width

The coded form of the regression equation for the response BW was found to be as follows:

$$\begin{aligned}\mathrm{BW}_{\mathrm{coded}} = {} & 4.50330 + 0.29119X_1 + 0.49422X_2 \\ & - 0.27003X_3 + 0.00973X_1^2 \\ & + 0.09896X_2^2 + 0.05508X_3^2 \\ & - 0.07919X_1X_2 - 0.08240X_1X_3 \\ & - 0.11774X_2X_3 \end{aligned} \quad (9)$$

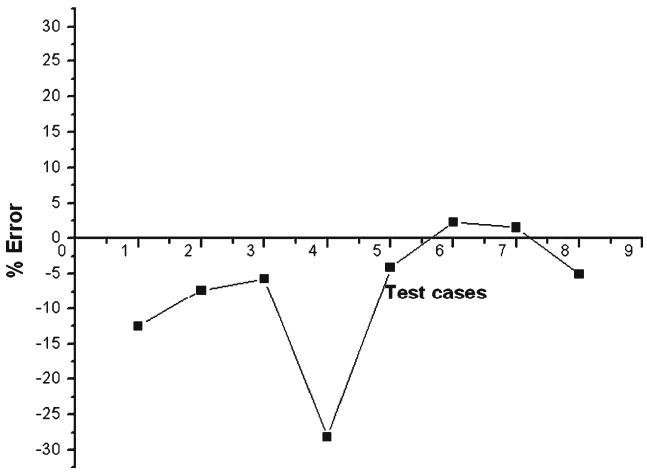

Fig. 6 Percent deviations in prediction of BP from the experimental values

Table 5 Significance test for BW

Sl. no.	Term	Coeff	SE coeff	T	p
1	Constant	4.50330	0.03800	118.496	0.000
2	X_1	0.29119	0.02809	10.368	0.000
3	X_2	0.49422	0.02809	17.597	0.000
4	X_3	−0.27003	0.02809	−9.614	0.000
5	X_1^2	0.00973	0.05426	0.179	0.859
6	X_2^2	0.09896	0.05426	1.824	0.075
7	X_3^2	0.05508	0.05426	1.015	0.316
8	X_1X_2	−0.07919	0.03140	−2.522	0.016
9	X_1X_3	−0.08240	0.03140	−2.624	0.012
10	X_2X_3	−0.11774	0.03140	−3.750	0.001

$S = 0.1538$ $R^2 = 93.0\%$ $R^2(\mathrm{adj}) = 91.5\%$

Analysis was carried out at a confidence level of 95%. The significance test of BW is shown in Table 5. The terms X_1, X_2, and X_3 were found to be significant. All the second-order terms were found to be insignificant, which clearly stated the prevalence of linear relationships. However, all the interaction effects like X_1X_2, X_2X_3, and X_3X_1 were seen to be significant. The coefficient of correlation was found to be equal to 0.93 for BW. Thus, the model was seen to be statistically adequate to make further predictions. The lack of fit was insignificant (refer to Table 6), and it implies that the insignificant terms could be removed from the model.

To interpret the inter-relationship amongst different operating parameters and BW, surface plots were plotted, as shown in Fig. 7. Figure 7a indicates that the bead width increased with the increase of both accelerating voltage as well as beam current. From Fig. 7b, it can be observed that BW increased with the increase in accelerating voltage and decrease in welding speed. The BW was also found to increase, when the welding was carried out at the higher beam current and lower welding speed, as shown in Fig. 7c. The un-coded form of the response equation related to BW, as shown in Eq. 10, was used to test its performance on eight test cases.

Table 6 ANOVA test for BW

Source	DF	Seq SS	Adj SS	Adj MS	F	p
Regression	9	12.9528	12.9528	1.43920	60.82	0.000
Linear	3	12.0587	12.0587	4.01958	169.86	0.000
Square	3	0.2479	0.2479	0.08264	3.49	0.024
Interaction	3	0.6462	0.6462	0.21539	9.10	0.000
Residual error	41	0.9702	0.9702	0.02366		
Lack-of-fit	5	0.2382	0.2382	0.04765	2.34	0.061
Pure error	36	0.7320	0.7351620	0.02033		
Total	50	13.9230				

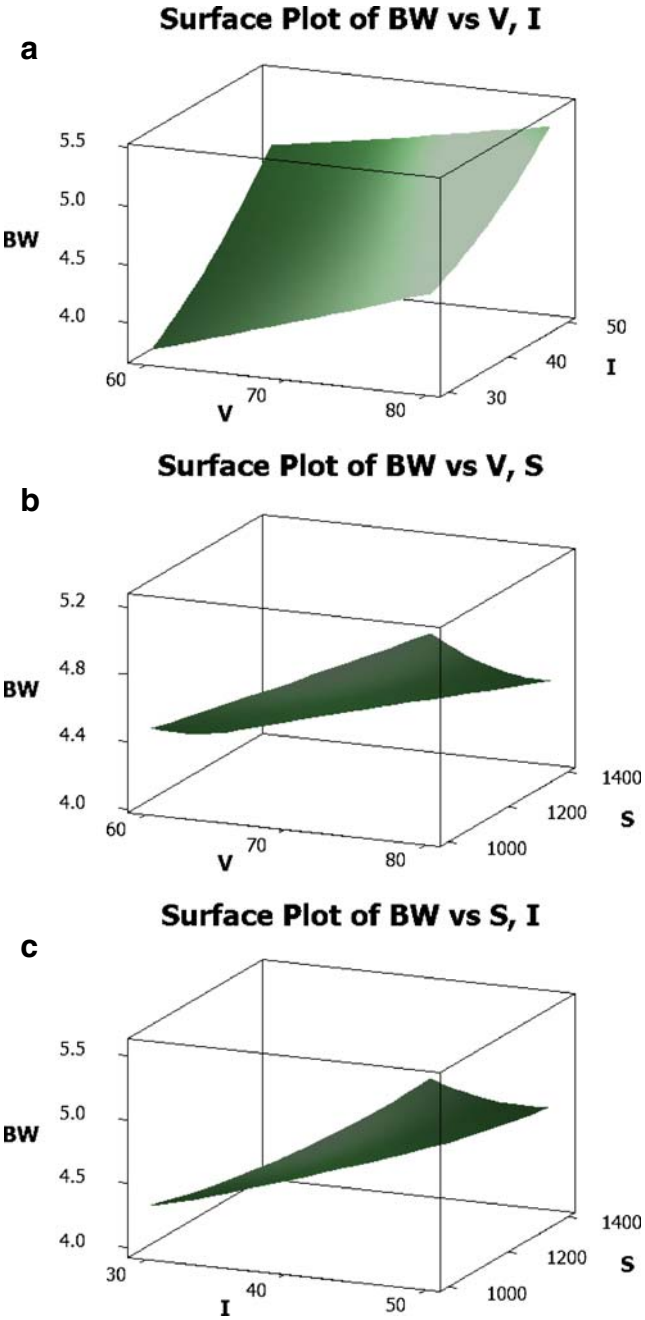

Fig. 7 Surface plots of BW with V, I, and S (**a**–**c**)

$$\begin{aligned}\mathrm{BW}_{\mathrm{un-coded}} = {} & -2.35266 + 0.0966160V + 0.0963347I \\ & + 0.000583644S + 0.0000972885V^2 \\ & + 0.000989569I^2 + 0.00000137708S^2 \\ & - 0.000791937VI - 0.0000412001VS \\ & - 0.0000588689IS \end{aligned} \tag{10}$$

The *MSD* in prediction of BW was found to be equal to 0.109277. Figure 8 shows the values of percent deviation in prediction of BW, which were found to lie in the range of −4.47% to 15.8%.

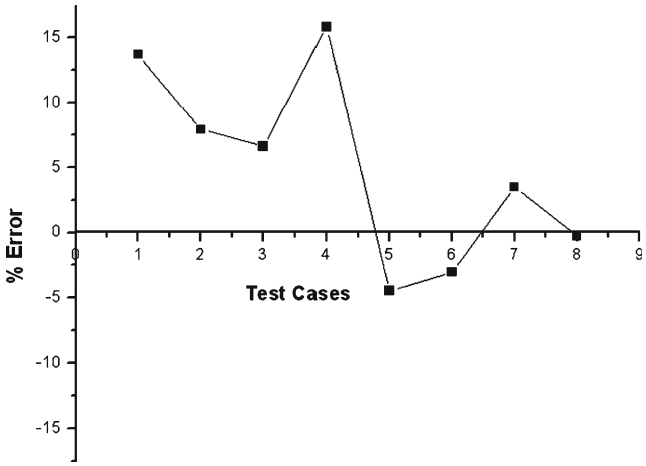

Fig. 8 Percent deviations in prediction of BW from the experimental values

In a similar way, the regression equations (represented by Eqs. 11 through 14) were developed for other co-ordinates, like a_1, b_1, a_2, and b_2. The correlation coefficients for the co-ordinates were found to be equal to 0.968, 0.995, 0.953, and 0.993, respectively.

$$\begin{aligned} a_1 = {} & -8.91098 + 0.306079V + 0.122215I \\ & - 0.00171240S - 0.00143017V^2 \\ & + 0.000586272I^2 + 0.0000018425S^2 \\ & - 0.00118376VI - 0.0000350917VS \\ & - 0.0000405610IS \end{aligned} \tag{11}$$

$$\begin{aligned} b_1 = {} & -10.9743 + 0.273702V - 0.214996I \\ & + 0.00438048S - 0.000688303V^2 \\ & + 0.00203828I^2 + 0.000000509135S^2 \\ & + 0.00315302VI - 0.000114171VS \\ & + 0.00000169463IS \end{aligned} \tag{12}$$

$$\begin{aligned} a_2 = {} & -1.99449 + 0.113778V + 0.136124I \\ & - 0.00205764S - 0.000113210V^2 \\ & + 0.000363211I^2 + 0.00000181982S^2 \\ & - 0.00108518VI - 0.0000320195VS \\ & - 0.0000358773IS \end{aligned} \tag{13}$$

Table 7 Optimized working parameters

Operator	Value
Accelerating voltage	80 kV
Beam current	50 mA
Welding speed	1,055.3 mm/min

Table 8 Optimized weld bead geometries

Bead width	5.7 mm
Bead penetration	10.4 mm

$$b_2 = -7.75613 + 0.112882V - 0.201489I + 0.00854328S + 0.000432734V^2 + 0.00205200I^2 - 0.00000166835S^2 + 0.00299155VI - 0.000104147VS + 0.00000517494IS \quad (14)$$

5.2 Optimization of bead geometry

The fitness of the binary-coded GA f was calculated as the area within the curves representing the weld-bead profile. The input variables were V, I, and S. As the performance of a GA is dependent on its operating parameters, a careful parametric study was conducted. The following GA parameters were found to give the best results: probability of mutation $p_m = 0.001$; population size $N = 100$; maximum number of generation $G = 50$. A uniform crossover with probability p_c equal

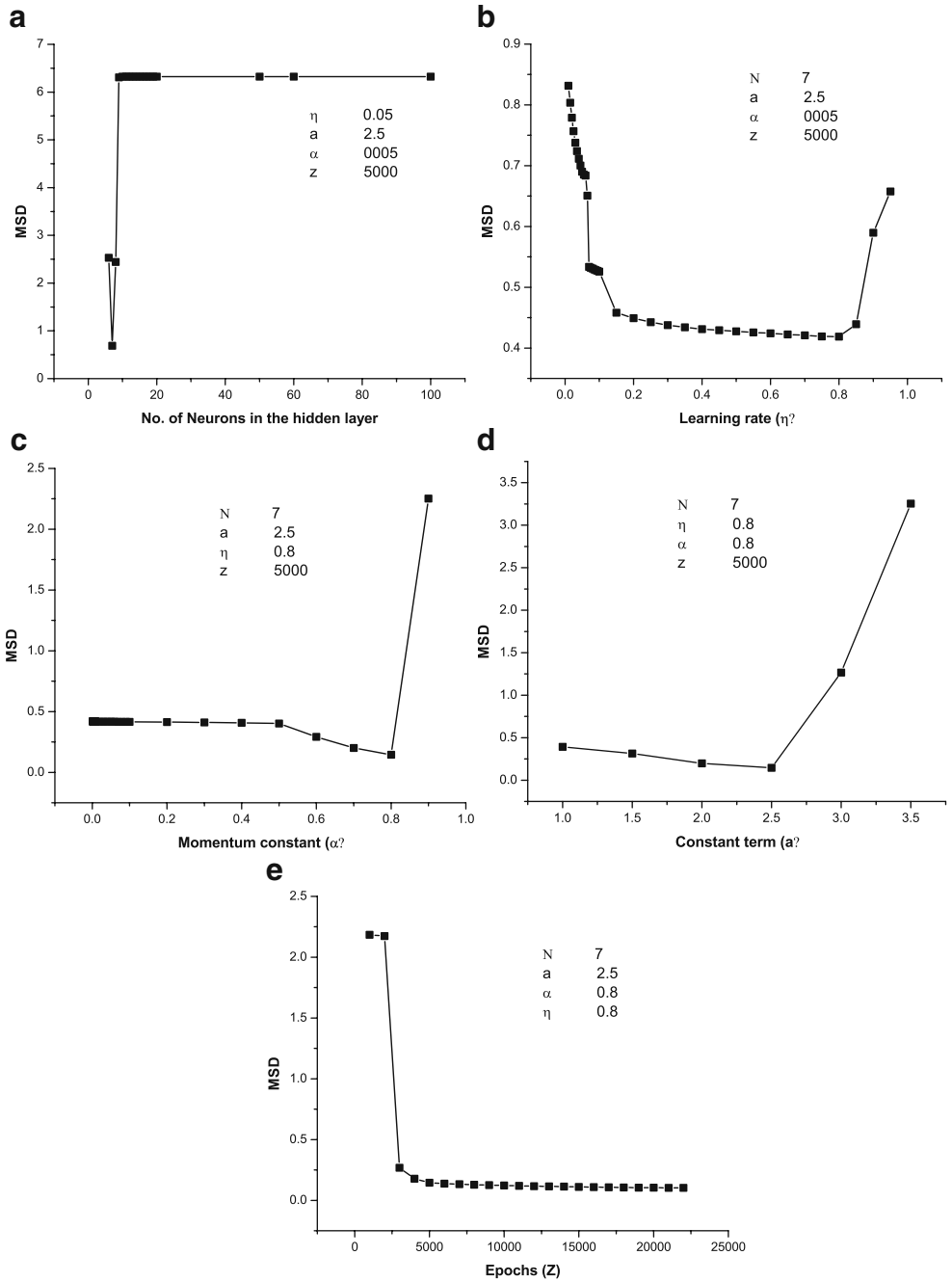

Fig. 9 Parametric study for BPNN (**a**–**e**)

to 0.5 was utilized for the said purpose. Through a careful study, the minimum value of BW (i.e., BW_{min}) and maximum value of BP (i.e., BP_{max}) were found to be equal to 3.7 and 10.4 mm, respectively. Moreover, the values of the variables: a, b, and C in Eq. 5 were found to be equal to 2, 40, and 1, respectively, through a detailed study. Thus, the penalty term P took the form shown below.

$$P = 1.0 \times \left[\left(\frac{BW}{3.7} \right)^2 + \left(\frac{10.4}{BP} \right)^{40} \right] \quad (15)$$

The optimal GA parameters were obtained through a thorough and careful study. The following GA parameters were found to yield the best results: $p_m = 0.0035$; $N = 100$; $G = 50$. A uniform crossover scheme was utilized for the said purpose.

The GA could find the minimum area of weldment as 28.6 mm^2. It was able to push the bead parameters like width and penetration towards their minimum and maximum values, respectively. A combination of the welding parameters shown in Table 7 could yield the desired weld geometries, as given in Table 8. However, it might be a difficult task to determine the most appropriate set of the above parameters, so that the GA could reach the globally minimum weldment area.

5.3 Bead profile prediction

The regression equations developed in Section 5.1 were utilized to generate 1,000 training cases at random by varying the input process parameters within their respective ranges. These were used to train both the BPNN and GA-NN separately. Details of the architectures and their results are discussed below.

5.3.1 Back-propagation neural network

A parametric study was carried out to determine the suitable parameters for neural network, in which one parameter was varied at a time, keeping the others unaltered. Figure 9 shows the results of the same. The number of neurons of the hidden layer, constant term—**a**, learning rate, momentum constant, and number of epochs were adjudged to be 7, 2.5, 0.8, 0.8, and 14,000, respectively. The same constant term **a** was used for the log-sigmoid transfer function in both the hidden

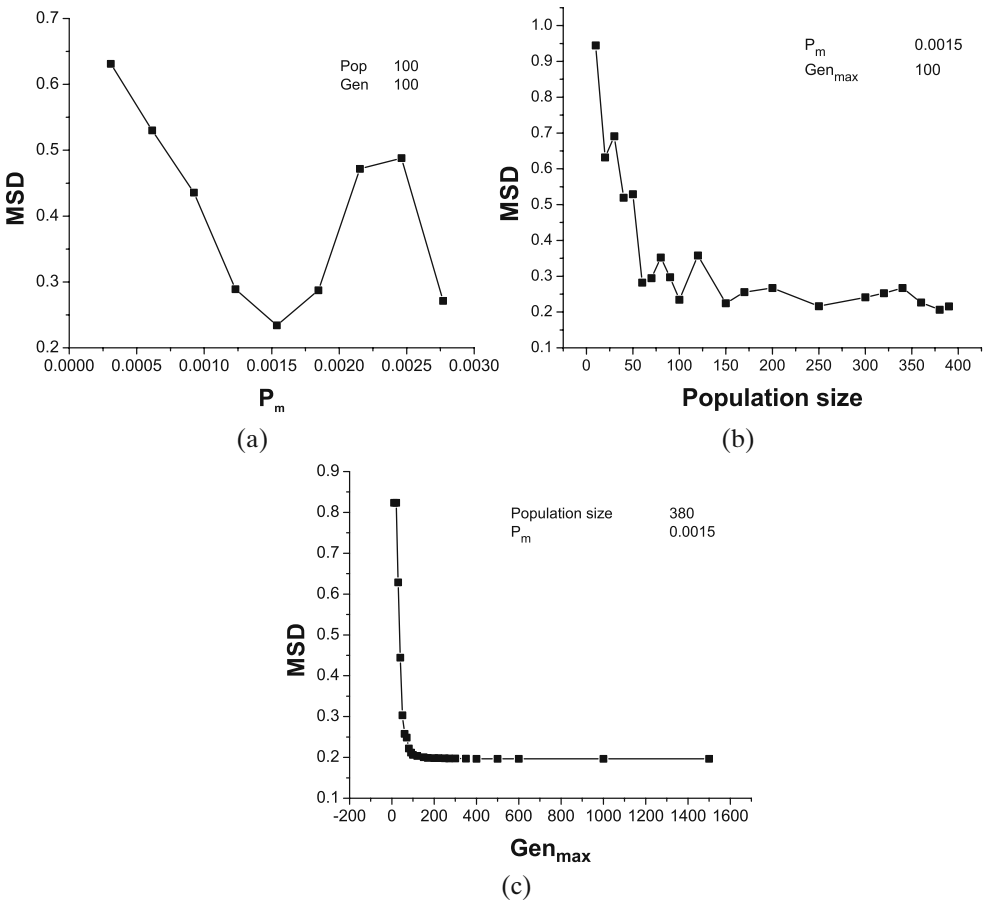

Fig. 10 Parametric study for GA-NN (**a**–**c**)

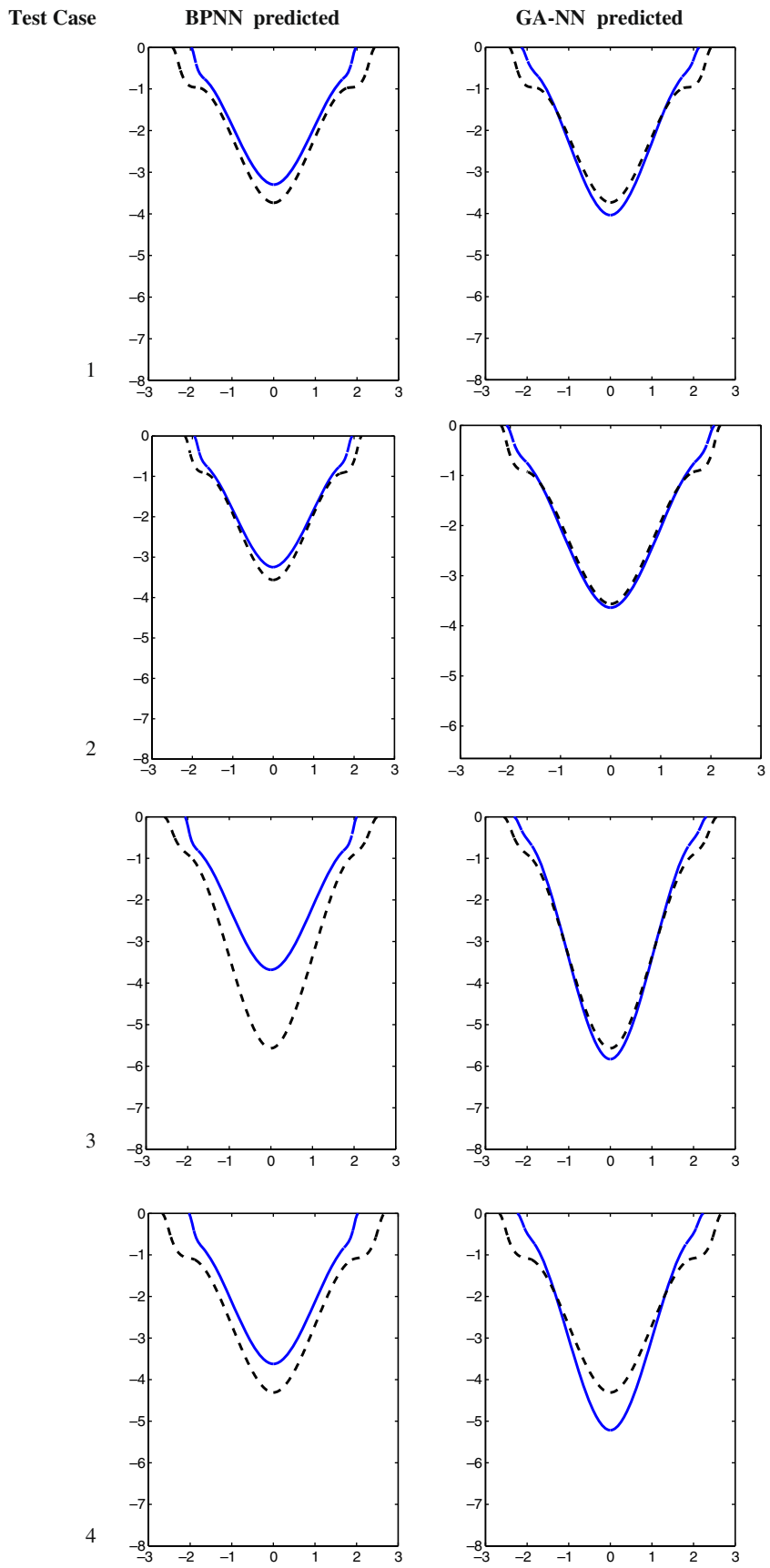

Fig. 11 Weld bead profiles predicted by the BPNN and GA-NN approaches

Fig. 11 (continued)

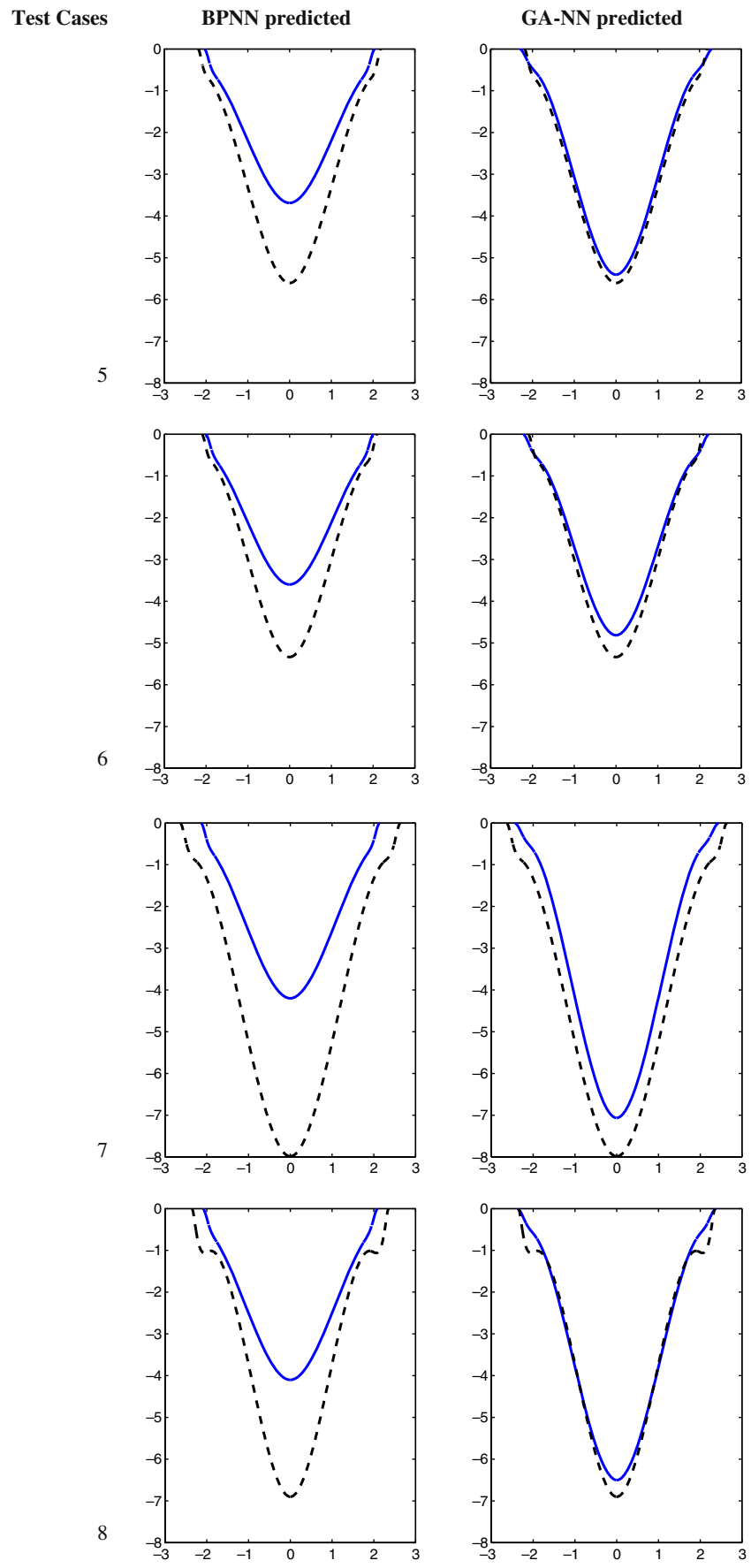

and output layers of the network. A back-propagation algorithm was used to train the neural network by following a batch mode of training.

5.3.2 Genetic-neural system

The back-propagation algorithm was replaced by a GA in this approach. The following GA parameters were found to yield the best results (obtained through a careful study, as shown in Fig. 10): $p_m = 0.0015$, population size = 380, number of generations = 300. A uniform crossover with probability $p_c = 0.5$ had been utilized.

5.3.3 Comparisons

After optimizing both of the networks, eight test cases were passed through them for performance evaluation. The outcomes of both of the networks were the coordinates of the points lying on the bead profile. These data were utilized in a Matlab script file, which generated the profiles. For each of eight test cases, BPNN- and GANN-predicted weld-bead profiles were compared with their respective actual profiles (refer to Fig. 11). The actual and predicted profiles were represented using black-dashed and blue lines, respectively. It is to be noted that the negative dimensions shown in the above figure indicate the direction of measurement only. The GA-NN was found to perform better than the BPNN in predicting the bead profiles. Being a gradient-based method, the chance of the back-propagation algorithm for being trapped into the local minima is greater. On the other hand, the probability of the GA solutions for getting stuck at the local minima is less. Thus, GA-NN was seen to outperform the BPNN in predicting the weld bead profile.

6 Concluding remarks

Bead-on-plate welding was carried out on Al-1100 plates as per central composite design of experiments. Regression analysis was conducted to determine input–output relationships of the process. A constrained optimization problem was formulated to minimize weldment area, after ensuring the condition of maximum bead penetration. A binary-coded GA with a penalty term was used to solve the said problem. The GA was able to reach near the globally optimal solution, after satisfying the above constraints. Weld-bead profiles had been predicted using the neural networks. The GA-NN was found to perform better than the BPNN. It might have happened due to the exhaustive search carried out by the GA in the GA-NN approach.

Acknowledgment The authors are grateful to Mr. Derose, Mr. Wilbert, and other supporting staff-members of CDM, Bhabha Atomic Research Centre, Mumbai, India, for their help in carrying out the experiments. They also acknowledge the sincere efforts of Dr. Krishnan, Head CDM, for providing the electron beam welding facility to conduct the experiments.

References

1. Dixon RD (1973) An accurate method for determining electron beam welding voltages. Weld J 52(8):343s–346s
2. Koleva E (2001) Statistical modelling and computer programs for optimisation of the electron beam welding of stainless steel. Vacuum 62:151–157
3. Koleva E (2005) Electron beam weld parameters and thermal efficiency improvement. Vacuum 77:413–421
4. Gunaraj V, Murugan N (1999) Prediction and comparison of the area of the heat affected zone for the bead-on-plate and bead-on-joint in submerged arc welding of pipes. J Mater Process Technol 95:246–261
5. Gunaraj V, Murugan N (2000) Prediction and optimization of weld bead volume for the submerged arc process—part 1. Weld J 78:286s–294s
6. Yang LJ, Bibby MJ, Chandel RS (1993) Linear regression equations for modeling the submerged-arc welding process. J Mater Process Technol 39:33–42
7. Ganjigatti JP, Pratihar DK, RoyChoudhury A (2007) Global versus cluster-wise regression analyses for prediction of bead geometry in MIG welding process. J Mater Process Technol 189:352–366
8. Benyounis KY, Olabi AG, Hashmi MSJ (2005) Effect of laser welding parameters on the heat input and weld-bead profile. J Mater Process Technol 164–165:978–985
9. Nagesh DS, Datta GL (2002) Prediction of weld bead geometry and penetration in shielded metal-arc welding ususing artificial neural networks. J Mater Process Technol 123: 303–312
10. De A, Jantre J, Ghosh PK (2004) Prediction of weld quality in pulsed current GMAW process using artificial neural network. Sci Technol Weld Join 9/3:253–259
11. Kim IS, Son JS, Park CE, Lee CW, Prasad YKDV (2002) A study on prediction of bead height in robotic arc welding using a neural network. J Mater Process Technol 130–131: 229–234
12. Lee JI, Um KW (2000) A prediction of welding parameters by prediction of back-bead geometry. J Mater Process Technol 108:106–113
13. Li P, Fang MTC, Lucas J (1997) Modelling of submerged arc weld beads using self-adaptive offset neural networks. J Mater Process Technol 71:288–298
14. Tay KM, Butler C (1997) Modelling and optimizing of a MIG welding process—a case study using experimental designs and neural networks. Qual Reliab Eng Int 13:61–70
15. Gunaraj V, Murugan N (2000) Prediction and optimization of weld bead volume for the submerged arc process—part 2. Weld J 78:331s–338s
16. Tarng YS, Yang WH (1998) Optimisation of the weld bead geometry in gas tungsten arc welding by the Taguchi method. J Adv Manufact Technol 14:549–554
17. Tarng YS, Juang SC, Chang CH (2002) The use of grey-based Taguchi mehtods to determine submerged arc welding process parameters in hard-facing. J Mater Process Technol 128:1–6

18. Olabi AG, Casalino G, Benyounis KY, Hashmi MSJ (2006) An ANN and Taguchi algorithms integrated approach to the optimization of CO_2 laser welding. Adv Eng Softw 37: 643–648
19. Kim D, Kang M, Rhee S (2005) Determination of optimal welding conditions with a controlled random search procedure. Weld J 83:125s–130s
20. Vasudevan M, Bhaduri AK, Baldev R, Rao KP (2007) Genetic algorithm based computational models for optimizing the process parameters of a TIG welding to achieve target bead geometry in type 304 L(N) and 316 L(N) stainless steels. Mater Manuf Process 22:641–649
21. Kumar A, Debroy T (2007) Tailoring fillet weld geometry using a genetic algorithm and a neural network trained with convective heat flow calculations. Weld J 92:26s–33s
22. Mishra S, Debroy T (2007) Tailoring gas tungsten arc weld geometry using a genetic algorithm and a neural network trained with convective heat flow calculations. Mater Sci Eng A 454–455:477–486
23. Kim D, Rhee S, Park H (2002) Modeling and optimization of a GMA welding process by genetic algorithm and response surface methodology. Int J Prod Res 40/7:1699–1711
24. Dutta P, Pratihar DK (2007) Modeling of TIG welding process using conventional regression analysis and neural network-based approaches. J Mater Process Technol 184: 56–68
25. Mollah AA, Pratihar DK (2008) Modeling of TIG welding and abrasive flow machining processes using radial basis function networks. Int J Adv Manufact Technol 37:9–10, 937–952
26. Kim IS, Son JS, Park CE, Kim IJ, Kim HH (2005) An investigation into an intelligent system for predicting bead geometry in GMA welding process. J Mater Process Technol 159: 113–118
27. Peretz R (1989) Weld cross-section profile prediction for deep penetration welding with laser beams. Opt Lasers Eng 11:27–48
28. Limmaneevichitr C, Kou S (2000) Experiments to simulate effect of marangoni convection on weld pool shape. Weld J 78/8:231s–237s
29. Robert A, Debroy T (2001) Geometry of laser spot welds from dimensionless numbers. Metall Mater Trans B 32B: 941–947
30. Dey V, Pratihar DK, Datta GL, Jha MN, Saha TK, Bapat AV (2009) Optimization of bead geometry in electron beam welding using a Genetic Algorithm. J Mater Process Technol 209:1151–1157
31. Holland JH (1975) Adaptation in natural and artificial systems. The University of Michigan Press, Ann Arbor
32. Chakraborti N (2004) Genetic algorithms in materials design and processing. Int Mater Rev 49/3–4:246–260
33. Pratihar DK (2008) Soft computing. Narosa, New Delhi